CONEM 2010
VI Congresso Nacional de Engenharia Mecânica
ABCM COMPROMETIDA COM A PROMOÇÃO DO DESENVOLVIMENTO DA ENGENHARIA E DAS CIÊNCIAS MECÂNICAS
ASSOCIAÇÃO BRASILEIRA DE ENGENHARIA E CIÊNCIAS MECÂNICAS
VI CONGRESSO NACIONAL DE ENGENHARIA MECÂNICA
VI NATIONAL CONGRESS OF MECHANICAL ENGINEERING
18 a 21 de agosto de 2010 – Campina Grande – Paraíba - Brasil
August 18 – 21, 2010 – Campina Grande – Paraíba – Brazil

A CFD ANALYSIS OF GAS-FLOW IN A SUPERSONIC EJECTOR

Thaís Piva de Castro, thapiva@ita.br[1]
Rosiane Cristina de Lima, rosiane.lima@vsesa.com.br[2]
Lincoln Nascimento Ribeiro, lincoln.ribeiro@uol.com.br[1]
Edson Luiz Zaparoli, zaparoli@ita.br[1]
Cláudia Regina de Andrade, claudia@ita.br[1]

[1]Instituto Tecnológico de Aeronáutica, Departamento de Engenharia Aeronáutica e Mecânica, Área de Aerodinâmica, Propulsão e Energia – Praça Marechal Eduardo Gomes, 50, Vila das Acácias, CEP 12.228-900, São José dos Campos, SP, Brasil.
[2]Vale Soluções em Energia S.A.– Rodovia Presidente Dutra, km 138, Eugênio de Melo, CEP 12.247-004, São José dos Campos, SP, Brasil.

Abstract: *In spite of ejector have low efficiency, it is attractive due to lack of moving parts, low cost and high reliability. Supersonic ejectors are widely used in different applications such as aerospace, propulsion and refrigeration. An ejector is a simple device since that it consists of four main unmoving components: primary nozzle, secondary inlet, mixing chamber and diffuser. Such pumps are characterized by the exchange of the kinetic energy of the primary fluid with the secondary fluid in a mixing chamber. In this work the mathematical model of this compressible flow is numerically solved using finite volume method with a coupled pressure-based approach. An adaptive mesh refinement is employed to capture shock reflections and shock-mixing layer interaction. Numerical results for the ejector pump efficiency was compared with available experimental literature data. Finally, it was done a numerical simulation varying the mass flow at the second inlet analyzing the increase pressure between the second inlet and diffuser outlet of a supersonic ejector.The simluation results shows that the increase pressure was reduced when the mass flow in second inlet was increased.*

Keywords*: ejector, supersonic, compressible, gas, CFD*

1. INTRODUCTION

The ejector was invented by Sir Charles Parsons around 1901, and in 1910 an ejector was used by Maurice Leblanc in the first steam jet refrigeration system. An ejector is a simple device since that it consists of four main unmoving components: primary nozzle, secondary inlet, mixing chamber and diffuser and is widely used in different applications such as aerospace, propulsion and refrigeration.

Most industrial processes use a significant amount of thermal energy, mostly by burning fossil fuels. Part of the energy released in combustion is rejected as waste. This waste heat can be utilized in certain types of refrigeration system such a jet refrigeration cycle that uses the ejector device. With the use of the ejector in refrigeration cycle, the amount of electricity purchased from utility companies, is reduced. Thus, utilization of the waste heat in refrigeration systems promotes mitigating the problems related to the environment, particularly by reduction of CO_2 emission from fossil fuels combustion in boilers of utility power plants, as cited in Chunnanond and Aphornratana (2004a).

Chunnanond and Aphornratana (2004b) performed experimental investigations of a refrigerator ejector for a better understanding of the flow and the mixing to increase the ejector efficiency. They examined the influences of the following operating conditions on the system performance: primary fluid superheated level and the position of the primary nozzle. It can be concluded that there are two parameters involved with the performance of a refrigerator ejector: the amount of secondary fluid passing through the mixing chamber, which determines the coefficient of performance (COP) and cooling capacity of the system and the momentum of the mixed stream, which indicates the critical condenser pressure. From the test, they concluded yet that decreasing boiler pressure, using a smaller nozzle and retracing the nozzle out of a mixing chamber can reduce the expansion angle of the expanded wave. Larger amounts of the secondary fluid can be entrained through the resultant longer and larger entrainement duct.

Bartosiewicz et al. (2005) performed numerical and experimental investigations to obtain a reliable hydrodynamics model of a supersonic ejector for refrigeration application. In the first part of their work, the performance of six turbulence models is evaluated in terms of correct representation of physical phenomena for supersonic ejectors and, in

the second part, the tested model was used to simulate the different operation modes of a supersonic ejector, ranging from on-design point to off-design. The work show that the RNG and sst - k – ω models were the best suited to predict the shock, strenght, and the mean line pressure recovery. However, the sst - k – ω model has shown better performances in term of stream mixing. The experimental apparatus utilized is illustrated in Fig. (1), where a screw compressor of sufficient capacity is used to ensure the continuous operation of the ejector. Compressed air is filtered to remove large particles such as dust and compressor oil droplets. The compressed air is then directed towards a reservoir, which is connected to the entrance of the ejector primary nozzle, just after a pressure control valve that adjust the primary stagnation pressure. The induced fluid is air taken from the surrounding atmosphere. The induced mass flow rate can be regulated by means of a valve located at the entrance of the aspiration duct.

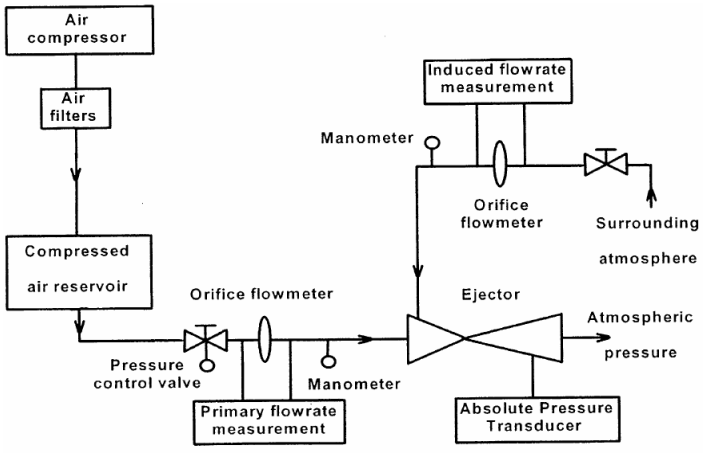

Figure 1. The schematic diagram of the experimental apparatus, Bartosiewicz et al. (2005).

Bartosiewicz et al. (2006) presented numerical results to supersonic ejector for refrigeration applications. CFD modeling was used to study the flow structure and operation under various operating conditions. This was the first paper dealing with local CFD modeling that takes into account shock–boundary layer interactions in a real refrigerant. The numerical results obtained, contribute to understanding the local structure of the flow and demonstrate the crucial role of the secondary nozzle for the mixing rate performance. They concluded that entrainment performance is mainly built in the secondary nozzle, while recompression is achieved in the mixing chamber. They concluded also that the strong shocks waves occurring at the secondary nozzle exit can dramatically decrease the mixing rate and even reverse the flow and the CFD software can predict ejector malfunction.

Sriveerakul et al. (2007a) presented a CFD analysis in order to predict the performance of a steam ejector used in refrigeration applications. This study was reported in two papers. In the first, Sriveerakul et al. (2007a), they investigated the effects of operating conditions and geometries on steam ejector and, in the second, Sriveerakul et al. (2007b), they concentrate on the use of CFD in visualizing the change in the flow structure and the mixing process inside the steam ejector as influenced by interested parameters, ejector's operating conditions and geometries. The CFD visualization shows two series of oblique shocks. The first series was found immediately after the primary fluid stream leaves the primary nozzle and begins to mix with the secondary fluid stream. The second series of oblique shock was found at the beginning of the diffuser section as a result of a non-uniform mixed stream. It can be seen that both entrainment ratio and critical back pressure can be varied simultaneously by adjusting three parameters, the primary fluid saturated pressure, the secondary fluid saturated pressure, and the primary nozzle size.

Ströher et al. (2007) presented a numerical study for compressible turbulent free jet. They tested different turbulence models using CFD to determine the most suitable model for the compressible overexpanded turbulent free jet. The results obtained from this investigation indicated that the sst- k- ω turbulence model produced better overall results.

In this work a study based on the experimental tests of Bartosiewicz et al. (2005) and Desevaux (2001) was numerically performed solving the mathematical model (continuity, momentum, energy, realizable k – ε or sst - k – ω turbulence model) using finite volume method, in order to investigate the ejector performance, analyzing the influence of the turbulence models and operation modes. The results numerically obtained are compared with the experimental results of Bartosiewicz et al. (2005).

2. PROBLEM DEFINITION

As described in Sriveerakul et al. (2007a), and shown in the Fig. (2), the primary fluid a high pressure and temperature expands and accelerates through the primary nozzle convergent-divergent (i), reaches sonic velocity in the throat and is ejected with supersonic velocity to create a very low pressure region at the primary nozzle exit (ii) and subsequently in the mixing chamber. This means "a secondary fluid" can be entrained into the mixing chamber. The speed of the secondary fluid rises to sonic value (iii) and chokes. Then the mixing process begins. This mixing causes the primary flow to be retarded whilst secondary flow is accelerated. By the end of the mixing chamber, the two streams are completely (iv). Due to a high pressure region downstream of the mixing chamber's throat, a normal shock of essentially zero thickness is induced (v). This shock causes a major compression effect and a sudden drop in the flow speed from supersonic to subsonic. A further compression of the flow is achieved (vi) as it is brought to stagnation through a subsonic diffuser.

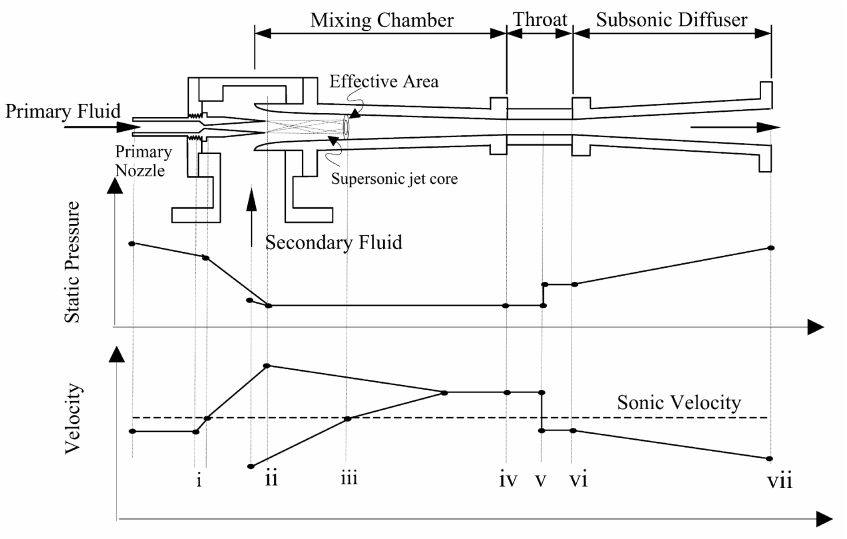

Figure 2. Schematic view and the variation of stream pressure and velocity as a function of location along a steam ejector, Sriveerakul et al. (2007a).

In this work, the geometrical configuration of the computational domain of a supersonic ejector was done according to the experimental setup of Bartosiewicz et al. (2005) and Desevaux (2001), shown in Fig. (3).

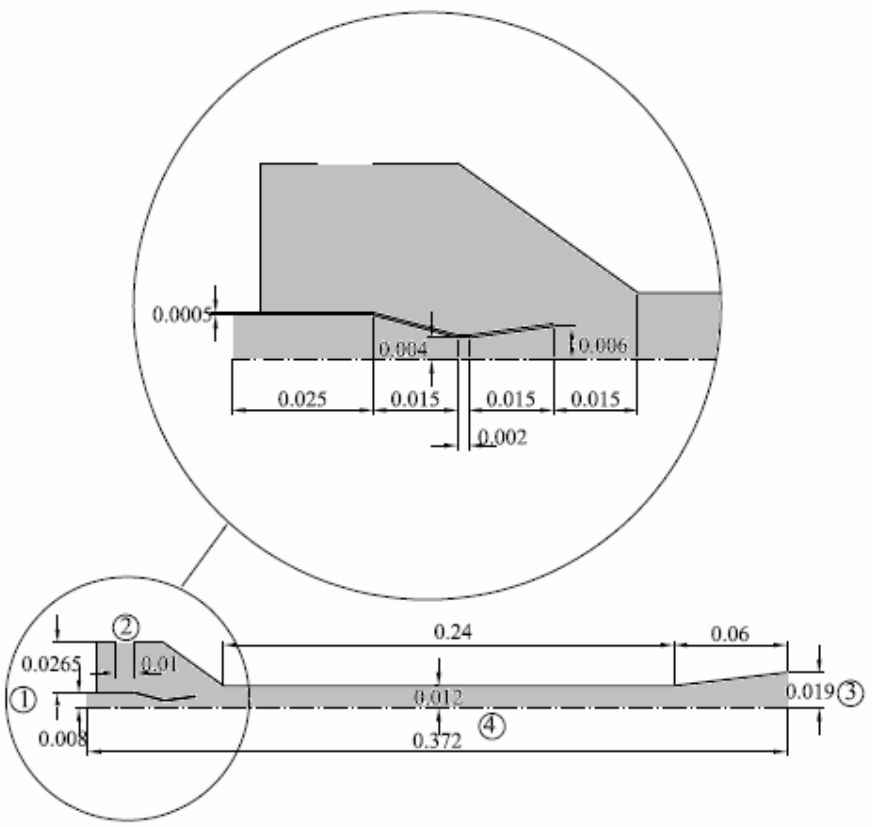

Figure 3. Geometric parameters of the supersonic ejector (dimensions in m).

3. MATHEMATICAL MODELING

The mathematical formulation can be described, in cartesian form, by continuity, momentum, energy and turbulence model equations (realizable – k– ε or sst – k– ω), Eqs. (1) to (9), respectively. Following assumptions were taken into account: two dimensional, axisymmetrical compressible ideal gas airflow, unsteady state regime and constants transport properties.

Continuity equation

$$\frac{\partial \rho}{\partial t} + \frac{\partial}{\partial x_i}(\rho u_i) = 0 \tag{1}$$

Momentum equation

$$\frac{\partial}{\partial t}(\rho u_i) + \frac{\partial}{\partial x_j}(\rho u_i u_j) = -\frac{\partial P}{\partial x_i} + \frac{\partial \tau_{ij}}{\partial x_j} \tag{2}$$

where stress tensor components are evaluated as:

$$\tau_{ij} = \left(\mu + \mu_t\right)\left(\frac{\partial u_j}{\partial x_i} + \frac{\partial u_i}{\partial x_j}\right) - \frac{2}{3}\left(\mu + \mu_t\right)\frac{\partial u_k}{\partial x_k}\delta_{ij}$$

Energy equation

$$\frac{\partial}{\partial t}(\rho E) + \frac{\partial}{\partial x_j}(u_j(\rho E + P)) = \frac{\partial}{\partial x_j}\left[\Gamma_E \frac{\partial T}{\partial x_j} + u_i(\tau_{ij})\right] \tag{3}$$

Equations of the realizable – k– ε model

$$\frac{\partial}{\partial t}(\rho k)+\frac{\partial}{\partial x_j}(\rho k u_j)=\frac{\partial}{\partial x_j}\left[\left(\mu+\frac{\mu_t}{\sigma_k}\right)\frac{\partial k}{\partial x_j}\right]+G_k-\rho\varepsilon-Y_M \tag{4}$$

$$\frac{\partial}{\partial t}(\rho \varepsilon)+\frac{\partial}{\partial x_j}(\rho \varepsilon u_j)=\frac{\partial}{\partial x_j}\left[\left(\mu+\frac{\mu_t}{\sigma_\varepsilon}\right)\frac{\partial \varepsilon}{\partial x_j}\right]-\rho C_2\frac{\varepsilon^2}{k+\sqrt{v\varepsilon}} \tag{5}$$

The constant values of the realizable k– ε model used in this work are: $\sigma_k=1.0$; $\sigma_\varepsilon=1.2$; $C_2=1.9$
The eddy viscosity is computed from:

$$\mu_t=\rho C_\mu\frac{k^2}{\varepsilon} \tag{6}$$

where

$$C_\mu=\frac{1}{A_0+A_S\dfrac{KU^*}{\varepsilon}};\ U^*\equiv\tilde{S}=\sqrt{S_{ij}S_{ij}};\ A_0=4.04;\ A_S=\sqrt{6}\cos\phi;\ \phi=\frac{1}{3}\cos^{-1}\left(\sqrt{6}W\right);\ W=\frac{S_{ij}S_{jk}S_{ki}}{\tilde{S}^3}$$

Equations of the sst - k– ω model

$$\frac{\partial}{\partial t}(\rho k)+\frac{\partial}{\partial x_i}(\rho k u_i)=\frac{\partial}{\partial x_j}\left[\left(\mu+\frac{\mu_t}{\sigma_k}\right)\frac{\partial k}{\partial x_j}\right]+\tilde{G}_k-Y_k \tag{7}$$

$$\frac{\partial}{\partial t}(\rho \omega)+\frac{\partial}{\partial x_i}(\rho \omega u_i)=\frac{\partial}{\partial x_j}\left[\left(\mu+\frac{\mu_t}{\sigma_\omega}\right)\frac{\partial \omega}{\partial x_j}\right]+G_\omega-Y_\omega \tag{8}$$

The constant values of the sst - k– ω model used in this work are: $\sigma_{k,1}=1.176$; $\sigma_{k,2}=1.0$; $\sigma_{\omega,1}=2.0$; $\sigma_{\omega,2}=1.168$; $\alpha_\infty^*=1$; $R_k=6$; $\beta_i=0{,}072$;
The turbulent viscosity is computed from:

$$\mu_t=\frac{\rho k}{\omega}\frac{1}{\max\left[\dfrac{1}{\alpha^*},\dfrac{SF_2}{a_1\omega}\right]} \tag{9}$$

where

$$\sigma_k=\frac{1}{F_1/\sigma_{k,1}+(1-F_1)/\sigma_{k,2}};\ \sigma_\omega=\frac{1}{F_1/\sigma_{\omega,1}+(1-F_1)/\sigma_{\omega,2}};$$

$$\alpha^*=\alpha_\infty^*\left(\frac{\alpha_0^*+R_{e_t}/R_k}{1+R_{e_t}/R_k}\right);\ R_{e_t}=\frac{\rho k}{\mu\omega};\ \alpha_0^*=\frac{\beta_i}{3};$$

$$F_1=\tanh\left(\phi_1^4\right);\ F_2=\tanh\left(\phi_2^2\right)$$

$$\phi_1=\min\left[\max\left(\frac{\sqrt{k}}{0.09\omega y'},\frac{500\mu}{\rho y^2\omega}\right),\frac{4\rho k}{\sigma_{\omega,2}D_\omega^+ y^2}\right];\ \phi_2=\max\left(\frac{\sqrt{k}}{0.09\omega y'},\frac{500\mu}{\rho y^2\omega}\right)$$

$$D_{\omega}^{+} = \max\left[2\rho\frac{1}{\sigma_{\omega,2}}\frac{1}{\omega}\frac{\partial k}{\partial x_j}\frac{\partial \omega}{\partial x_j}, 10^{-10}\right];$$

Table 1. Symbols.

C_2 ;	constant of the k - ε model
G_k and $\tilde{G}_k$;	generation of turbulence kinetic energy due to the mean velocity gradients
G_{ω};	represents the generation of ω
P ;	Pressure
S_{ij} ;	Mean strain rate $S_{ij} = \frac{1}{2}\left(\frac{\partial u_j}{\partial x_i} - \frac{\partial u_i}{\partial x_j}\right)$
T ;	Temperature
U^* ;	mean velocity
Y_M ;	the contribution of the fluctuating dilatation in compressible turbulence to the overall dissipation rate
Y_k and Y_{ω} ;	dissipation of k and ω due to turbulence
k ;	turbulence kinetic energy
v ;	kinematic viscosity
ε ;	dissipation rate
μ ;	molecular dynamic fluid viscosity
ρ ;	fluid density
μ_t ;	turbulent dynamic fluid viscosity
ω :	specific dissipation rate
σ_k , σ_{ε} and σ_{ω} ;	turbulent Prandtl numbers for (k), (ε) and (ω), respectively
$\Gamma_E = \Gamma + \Gamma_T$;	effective thermal conductivity
i, j, k ;	space components

Boundary conditions

At surface 1, Fig. (3), or primary fluid inlet, the total pressure and total temperature, and normal flow direction to input surface are prescribed. At surface 2, secondary fluid inlet, total temperature and mass flow rate are prescribed, and in the outlet 3, or exit, the static pressure is fixed. At all inlet boundaries, 5% for turbulent intensity and 5 for turbulent viscosity ratio are specified, while, axis boundary condition is prescribed at surface 4. All the walls are considered to be adiabatic with no slip and enhanced wall law are used as turbulence model boundary conditions. Numerical values for inlet and outlet boundary conditions are shown in Tab. (2).

Table 2. Surfaces, boundary condition type, boundary conditions and values.

Surfaces	Boundary condition type	Prescribed Boundary Values	
1	Pressure inlet	T_{Total} = 300 K	P_{Total} = 4; 5atm
2	Mass flow rate	T_{Total} = 300 K	$\dot{m}$ = 0.020; 0.024; 0.028; 0.030; 0.032; 0.036; 0.040; 0.044; 0.048 kg/s
3	Pressure outlet	T_{Total} = 300 K	P_{static} = 1 atm

4. COMPUTATIONAL STRATEGY

The numerical simulations have been performed using the commercial CFD package FLUENT (12.1) that is based on finite volume methods (FVM). The compressible, turbulent, axisymmetric, steady flow was calculated using a pseudo-transient technique with a densitty based approach**.** The turbulence models utilized were realizable – k–ε or sst –k – ω. The transient formulation is first order implicit. Two numerical approximations were evaluated, first and second order for the advective terms and pressure. During algebraic equations system iterative solution, CFL is set to 1.

5. RESULTS

In these simulations, the domain shown in Fig. (3) was used, that is based on the experimental setup of Bartosiewicz et al. (2005) and Desevaux (2001).

Firstly, it has been done a validation comparing with Bartosiewicz et al. (2005) results to analyse the effect of convective terms discretization schemes, first and second order, and the performance of realizable – k– ε or sst – k– ω turbulence models. For these tests, there is no secondary flow, the inlet pressure is $P_{Total\ =}$ 5 atm, all the graphics are plotted from the primary nozzle outlet and $P_{r\ =}$ 5 atm is taken as a reference .

Figure (4) and the Fig. (5) illustrate the results for the axial pressure obtained with two different discretization schemes and realizable – k– ε or sst – k– ω turbulence model respectively, comparing the results of this present work to numerical and experimental results of Bartosiewicz et al. (2005). The discretization scheme results that better agree with measurements is the first order for both turbulence models.

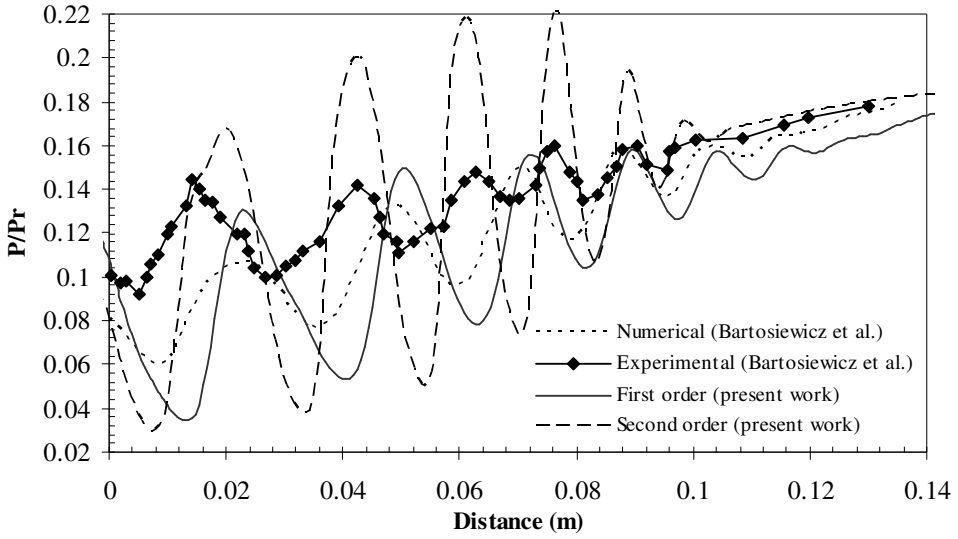

Figure 4. Realizable – k– ε model axial pressure results for no secondary flow.

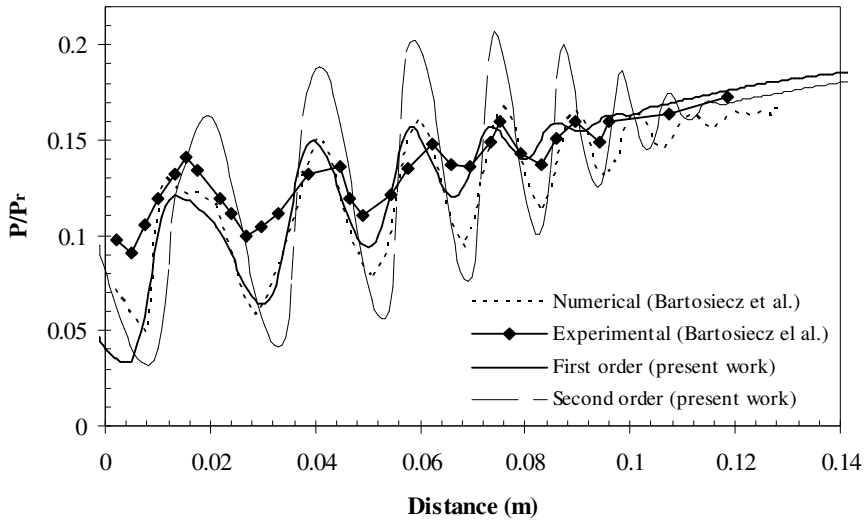

Figure 5. sst – k– ω model axial pressure results for no secondary flow.

Figure (6) illustrates results for the axial pressure obtained with realizable – k– ε or sst – k– ω turbulence model and also the experimental ones of Bartosiewicz et al. (2005). Performance of sst – k– ω turbulence model is better than realizable – k– ε for ejector modeling. Based in this comparison, sst – k– ω turbulence model was used obtain following results.

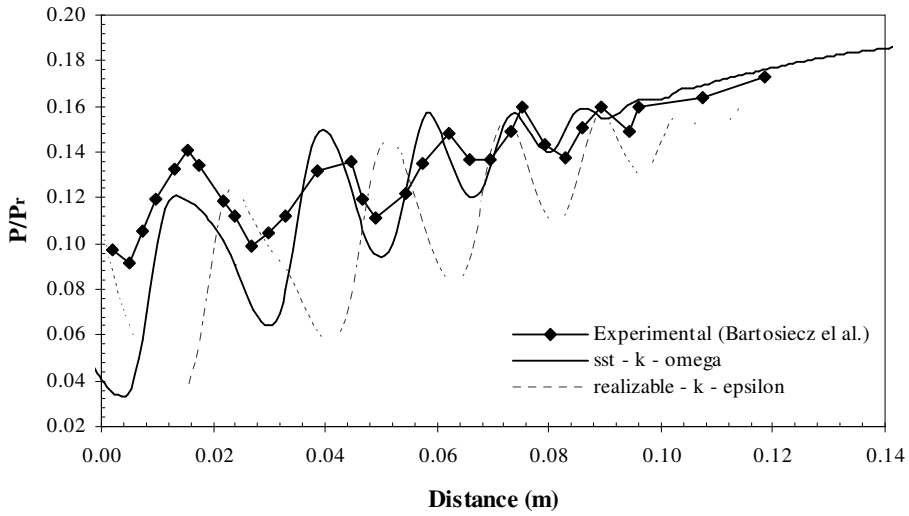

Figure 6. Comparison between the sst – k– ω and the realizable – k– ε model with first order discretization scheme for no secondary flow.

In Fig. (7), a comparison with Bartosiewicz et al. (2005) results. In present work numerical results were obtained with convective terms first order discretization and sst – k– ω turbulence model for an ejectorwith induced secondary flow ($\dot{m}$ = 0.028 kg/s) For this case, the primary flow inlet pressure was P_{Total} = 4atm. There was a shift in the first pressure oscilation, however, this phase difference was reduced for posterior oscilations. Numerical results present more oscilations than experimental ones.

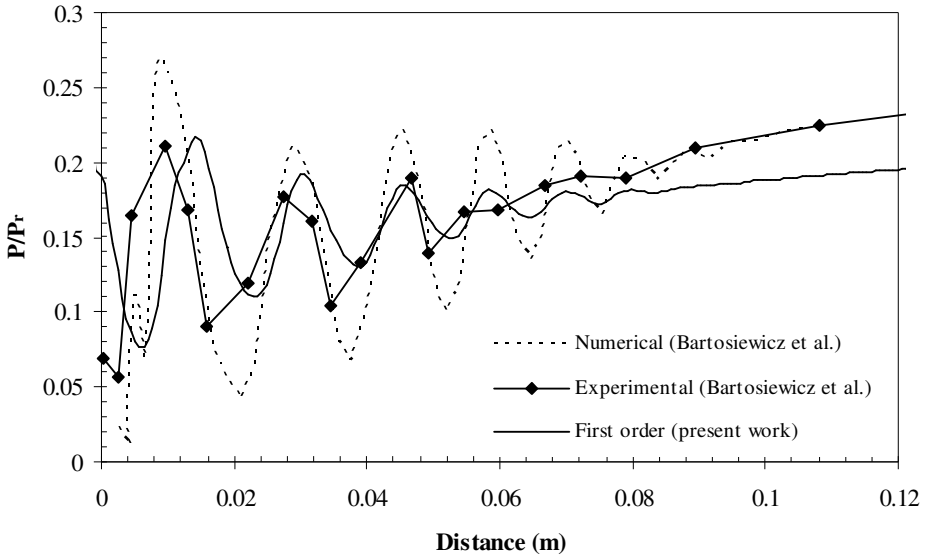

Figure 7. Axial pressure sst – k– ω model with secondary flow.

To evaluate secondary mass flow in the supersonic ejector performance, a simulation using sst – k - ω turbulence model was done. Results was shown in Fig. (8), it is possible to see a reduction in the pressure increase (P_3-P_2) as secondary mass flow rate increases.

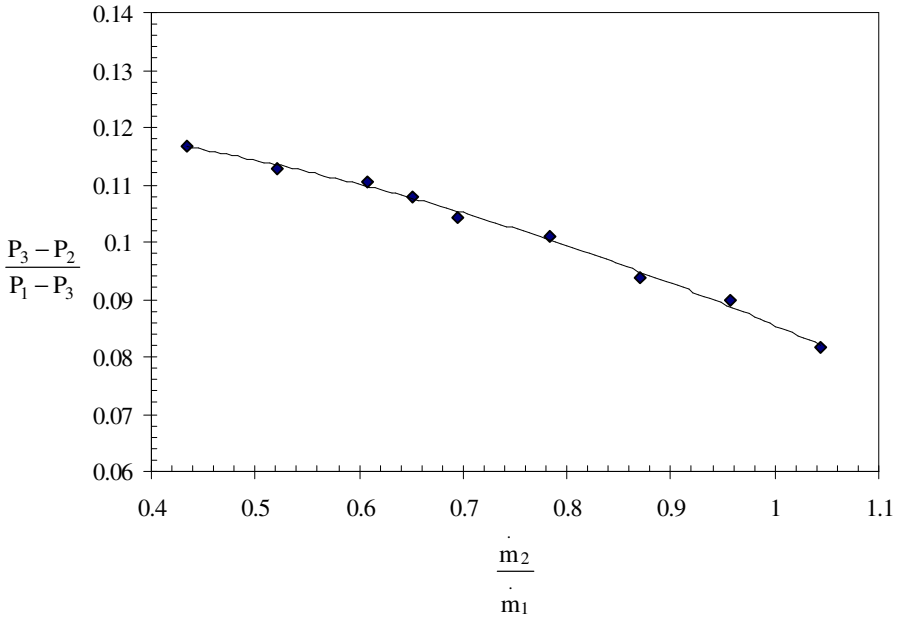

Figure 8. Supersonic ejector performance.

6. CONCLUSION

In this work it was performed a numerical simulation to analyze the performance of supersonic ejector varying the secondary mass flow rate. Two discretization schemes (first and second order) and two turbulence models (realizable k- ε and sst-k-ω turbulence models) were tested. The better agreement with experimental results of Bartosiewicz (2005) was obtained using first order discretization scheme together sst-k-ω turbulence model.

For two cases studied (ejector with secondary flow and primary flow only) sst- k- ω turbulence model results shown better agreement with experimental results using first order convective terms discretization. There was a greater shift differences in the first pressure oscilation that is reduced for posterior cycles.

7. ACKNOWLEDGEMENTS

The authors would like to acknowledge the CAPES by the financial support and the GSET (Group of Simulation of Flow and Heat Transfer) by the computational support.

8. REFERENCES

Bartosiewicz, Y., Aidoun, Z., Desevaux, P. and Mercadier, Y., 2005, "Numerical and experimental investigations on supersonic ejectors" , Int. J. of Heat and Fluid Flow, Vol. 26, pp. 56-70.

Bartosiewicz, Y., Aidoun, Z. and Mercadier, Y., 2006, "Numerical assessment of ejector operation for refrigeration applications based on CFD", Applied Thermal Engineering, Vol. 26, pp. 604-612.

Chunnanond, K. and Aphornratana, S., 2004a, "Ejectors: aplications in refrigeration technology", Renewable and Sustainable Energy Reviews, Vol. 8, pp. 129-155.

Chunnanond, K. and Aphornratana, S., 2004b, "An experimental investigation of a steam ejector refrigerator: the analysis of the pressure profile along the ejector", Applied Thermal Engineering, Vol. 24, pp. 311-322.

Desevaux, P., 2001, "A method for visualizing the mixing zone between two co-axial flows in an ejector", Optics and Lasers in Engineering, Vol. 35, pp. 317-323.

Fluent Inc. Theory Guide, 2008, 12.0 version.

Sriveerakul, T., Aphornratana, S. and Chunnanond, K., 2007a, "Performance prediction of steam ajector using computational fluid dynamics: Part 1. Validation of the CFD results", Int. J. of Thermal Sciences, Vol. 46, pp. 812-822.

Sriveerakul, T., Aphornratana, S. and Chunnanond, K., 2007b, "Performance prediction of steam ajector using computational fluid dynamics: Part 2. Flow structure of a steam ejector influenced by operating pressures and geometries", Int. J. of Thermal Sciences, Vol. 46, pp. 823-833.

Ströher, G. R., Zaparoli, E. L. and Andrade, C. R., 2007, "Numerical Study of Axisymmetric compressible turbulent free jet problem", XXVIII Iberian Latin-American Congress on Computational Methods in Engineering, Porto, Portugal. Proceedings of the 28th Iberian Latin-American Congress on Computational Methods in Engineering. ABMEC, 2007.

9. RESPONSIBILITY NOTICE

The author(s) is (are) the only responsible for the printed material included in this paper.